JOURNAL OF GEOPHYSICAL RESEARCH, VOL. 113, D20312, doi:10.1029/2008JD009820, 2008

Predicted impacts of climate and land use change on surface ozone in the Houston, Texas, area

Xiaoyan Jiang,[1] Christine Wiedinmyer,[2] Fei Chen,[2] Zong-Liang Yang,[1] and Jeff Chun-Fung Lo[1]

Received 13 January 2008; revised 16 July 2008; accepted 5 August 2008; published 30 October 2008.

[1] This paper studies the effects of climate change under future A1B scenario and land use change on surface ozone (O_3) in the greater Houston, Texas, area. We applied the Weather Research and Forecasting Model with Chemistry (WRF/Chem) to the Houston area for August of current (2001–2003) and future (2051–2053) years. The model was forced by downscaled 6-hourly Community Climate System Model (CCSM) version 3 outputs. High-resolution current year land use data from National Land Cover Database (NLCDF) and future year land use distribution based on projected population density for the Houston area were used in the WRF/Chem model coupled with an Urban Canopy Model (UCM). Our simulations show that there is generally a 2°C increase in near-surface temperature over much of the modeling domain due to future climate and land use changes. In the urban area, the effect of climate change alone accounts for an increase of 2.6 ppb in daily maximum 8-h O_3 concentrations, and a 62% increase of urban land use area exerts more influence than does climate change. The combined effect of the two factors on O_3 concentrations can be up to 6.2 ppb. The impacts of climate and land use change on O_3 concentrations differ across the various areas of the domain. The increase in extreme O_3 days can be up to 4–5 days in August, in which land use contributes to 2–3 days' increase. Additional sensitivity experiments show that the effect of future anthropogenic emissions change is on the same order of those induced by climate and land use change on extreme O_3 days.

Citation: Jiang, X., C. Wiedinmyer, F. Chen, Z.-L. Yang, and J. C.-F. Lo (2008), Predicted impacts of climate and land use change on surface ozone in the Houston, Texas, area, *J. Geophys. Res.*, *113*, D20312, doi:10.1029/2008JD009820.

1. Introduction

[2] High levels of surface ozone (O_3), one of major air pollutants in the lower troposphere, have detrimental effects on human health and plants. The conditions conducive to high O_3 concentrations near the surface generally include warm weather, high solar radiation and high-pressure systems. Future continuing increase in the average global temperature as predicted by most climate models, together with future land use change induced by human activities [*Intergovernmental Panel on Climate Change* (*IPCC*), 2007] may exert a strong influence on future surface O_3 air quality. It is of primary interest to examine future air quality change in response to future changes in climate and land use, to help policy makers set future national air quality standards such as the National Ambient Air Quality Standard (NAAQS) in the United States.

[3] In recent years, efforts have been put into estimating future changes in surface O_3 concentrations due to changes in future anthropogenic emissions and climate change on global and regional scales [e.g., *Prather et al.*, 2003; *Hogrefe et al.*, 2004; *Mickley et al.*, 2004; *Leung and Gustafson*, 2005; *Forkel and Knoche*, 2006; *Murazaki and Hess*, 2006; *Racherla and Adams*, 2006; *Tao et al.*, 2007; *Tagaris et al.*, 2007]. *Prather et al.* [2003] summarized the projected future changes in O_3 on a global scale on the basis of 10 global models. Yet their study only considers changes in O_3 due to changes in anthropogenic emissions. *Hogrefe et al.* [2004] reported the first study that applied a modeling system consisting of a global climate model, a regional climate model, and an air quality model to estimate the potential effects of future climate change on surface O_3 over the eastern United States. More recently, *Tagaris et al.* [2007] estimated the impacts of future global climate change and emissions change on U.S. O_3 concentrations; their results revealed that climate change, alone, with no emissions change had a small effect on the maximum 8-h O_3 concentrations. *Tao et al.* [2007] investigated the relative contributions of projected future emissions change and climate change to surface O_3 concentrations in the United States. The results of their study showed that the magnitude of changes in surface O_3 concentrations differed in metropolitan and rural areas. However, in these studies, future urban land use change in metropolitan areas is not included.

[1] Department of Geological Sciences, John A. and Katherine G. Jackson School of Geosciences, University of Texas at Austin, Austin, Texas, USA.
[2] National Center for Atmospheric Research, Boulder, Colorado, USA.

0148-0227/08/2008JD009820$09.00

[4] As more land area in metropolitan regions is expected to be converted from natural and vegetated land cover to human-dominated uses in the future, resulting changes in air temperature, wind field, humidity and height of the atmosphere boundary layer induced by land use change [*Civerolo et al.*, 2000; *Grossman-Clarke et al.*, 2005; *Liu et al.*, 2006; *Lo et al.*, 2007] can affect the production and distribution of air pollutants [*Taha*, 1996; *Taha et al.*, 1998; *Civerolo et al.*, 2007; *Wang et al.*, 2007]. It has been demonstrated that the spatial patterns of air pollutants were positively correlated with urban built-up density [*Weng et al.*, 2006], indicating the requirement of better treatments of urban features in the numerical models. By refining a land use classification for the arid Phoenix metropolitan area and introducing a bulk approach to a mesoscale atmospheric model, *Grossman-Clarke et al.* [2005] found that the model with the new features can better simulate the daytime part of the diurnal temperature cycle in the urban area, which can improve the simulation of surface O_3 levels in air quality models.

[5] Despite the recognition that land use change can have significant impacts on modeled meteorology and air quality, most of the previous studies generated future regional climate variables to drive the air quality models without any adjustments to the land use patterns [e.g., *Hogrefe et al.*, 2004; *Tao et al.*, 2007]. The exception of work includes *Civerolo et al.* [2007], who applied future land use data estimated by a land use change model to one climate scenario to explore the effects of increased urbanization on surface O_3. However, in their work, they used global climate model outputs, a regional climate model along with an offline photochemical model. The treatment for urban land use categories in their study was very simple, through assigning several new parameters for three urban land use types which were classified on the basis of vegetation fraction. As detailed Urban Canopy Models (UCMs) have been developed [e.g., *Kusaka et al.*, 2001; *Kusaka and Kimura*, 2004a, 2004b; *Holt and Pullen*, 2007], we are able to better understand the contribution of urbanization to changes in near-surface O_3 from the modeling perspective.

[6] Under the Clean Air Act, the Houston–Galveston–Brazoria (HGB) area is classified as an O_3 nonattainment area, which could be attributed to its rapid urban development, extensive sources of anthropogenic emissions, unique land use and land cover patterns, and complex coastal zones. Most of the previous studies have been focused on the impacts of anthropogenic [e.g., *Jiang and Fast*, 2004; *Tao et al.*, 2004; *Fast and Heilman*, 2005; *Nam et al.*, 2006] and biogenic emissions [e.g., *Byun et al.*, 2005; *Li et al.*, 2007] and meteorological conditions [e.g., *Dabberdt et al.*, 2004; *Zhang et al.*, 2007] on O_3 formation [*Jimenez et al.*, 2006; *Bossioli et al.*, 2007]. To date, no work has been done to assess the impacts of future climate change and land use change on the surface O_3 over the Houston area. The recent development of a fully coupled land-atmosphere-chemistry model with a detailed UCM allows us to assess the impacts of both climate change and land use change on air quality on regional scales simultaneously. In this study, results are presented for a modeling study aimed at predicting future changes in surface O_3 concentrations over the greater Houston area, taking into account the effects of climate change and land use change. We begin in section 2 with a brief description of the methods used in this study. In section 3, we compare model results with observations for present-day conditions, and discuss the contributions of future climate change and land use change to surface O_3 changes in the Houston area. Additionally, the results of sensitivity simulations concerning the contribution of anthropogenic emissions change to changed surface O_3 over the Houston area are presented.

2. Methodology

2.1. Regional Land-Atmosphere-Chemistry Model

[7] The physically based Weather Research and Forecasting Model [*Skamarock et al.*, 2005] with Chemistry (WRF/Chem) is a new-generation atmosphere-chemistry model developed collaboratively among several groups including the National Center for Atmospheric Research (NCAR) and the National Oceanic and Atmospheric Administration (NOAA) [*Grell et al.*, 2005]. The computations of meteorology and atmospheric chemistry in the WRF/Chem model share the same land surface schemes, time transport schemes, vertical mixing parameterizations, and time steps for transport and vertical mixing. It has been successfully applied for regional air quality studies [e.g., *Fast et al.*, 2006].

[8] Similar to the WRF model, the WRF/Chem model permits the choice between different physics and chemistry options. The following options were applied for the simulations presented here: Grell cumulus scheme [*Grell et al.*, 1994], WSM 5-class microphysics scheme [*Hong et al.*, 2004], Yonsei University Planetary Boundary Layer (PBL) scheme [*Hong and Pan*, 1996], Simple Cloud Interactive Radiation scheme [*Dudhia*, 1989] and Rapid Radiative Transfer Model longwave radiation scheme [*Mlawer et al.*, 1997]. The Regional Acid Deposition Model version 2 (RADM2) chemical mechanism [*Stockwell et al.*, 1990] was used to simulate gas phase chemistry. Several previous studies [e.g., *Tie et al.*, 2001; *Martin et al.*, 2003] suggest that the net effect of aerosols over the United States results in only a small decrease in O_3. Therefore, we did not include aerosol-induced changes in photolysis rates. The photolysis frequencies for the 21 photochemical reactions of the gas phase chemistry model are calculated at each grid point according to *Madronich* [1987].

[9] We used the Noah land surface model (LSM) [*Chen and Dudhia*, 2001; *Ek et al.*, 2003] coupled with an UCM in the WRF/Chem model. The Noah LSM calculates surface sensible heat flux, latent heat flux, and skin temperature for natural surfaces. The UCM is coupled to the Noah LSM through urban surface fractions [*Kusaka et al.*, 2001; *Kusaka and Kimura*, 2004a, 2004b]. This WRF/Noah/UCM coupled modeling system [*Chen et al.*, 2004, 2006] calculates the surface fluxes from man-made surfaces and includes the following: (1) 2-D street canyons that are parameterized to represent the effects of urban geometry on urban canyon heat distribution; (2) shadowing from buildings and reflection of radiation in the canopy layer; (3) the canyon orientation and diurnal cycle of the solar azimuth angle; (4) man-made surfaces consisting of eight canyons with different orientations; (5) Inoue's model for canopy flows [*Inoue*, 1963]; (6) the multilayer heat equation for the roof, wall, and road interior temperatures; and (7) a very thin bucket model for evaporation and runoff from road surfaces. To run the UCM within the Noah LSM for

Table 1. Surface Parameterizations for Each Land Use Category

Urban Type	Urban Fraction	Building Height (m)	Roughness Length (m)	Sky View Factor	Building Volumetric Parameter (m^{-1})	Normalized Building Height (m)	Anthropogenic Heat (cal cm^{-1} cm^{-1})
Industrial or commercial	0.95	10.	1.0	0.48	0.4	0.50	90.0
High-intensity residential	0.9	7.5	0.75	0.56	0.3	0.40	50.0
Low-intensity residential	0.5	5.	0.5	0.62	0.2	0.30	20.0

the Houston area, additional parameters such as building height, roughness length, sky view factor and anthropogenic heat for three land use categories (industrial or commercial, low-intensity residential, and high-intensity residential) are included in an additional lookup table. In general, the industrial or commercial land use category has higher building height, roughness length, and anthropogenic heat, and a lower sky view factor. The parameters for the three different urban land use types in the UCM are presented in Table 1. To conduct future year simulations, one problem is the specification of anthropogenic heating in cities. Because of the steady increase in energy consumption and the growth of cities, anthropogenic heating would change significantly in the future. One sensitivity experiment shows that the effect of anthropogenic heating only leads to a 0.6 ppb increase in O_3, which is not very significant. So in our future year simulations, we applied the same anthropogenic heating rate as in current year simulations.

2.2. Global and Regional Climate Modeling

[10] Current and future year regional climate fields were obtained by downscaling the NCAR Community Climate System Model version 3 (CCSM3) outputs, which have been used for the IPCC Fourth Assessment Report (AR4) [*Collins et al.*, 2006], to the regional scale. The horizontal resolution of CCSM3 is T85 ($\sim$1.41°). The greenhouse gas concentrations during the CCSM3 simulation period used in this study follow the IPCC Special Report on Emission Scenarios (SRES) A1B [*IPCC*, 2001], with increasing trace gases and aerosol concentrations from 2001 until 2050. The A1B scenario is a midline scenario for carbon dioxide output and economic growth; the predicted carbon dioxide emissions increase until around 2050 and then decrease after that. A full analysis of the CCSM3 future climate simulation is described by *Meehl et al.* [2006]. In this study, we simulated a control period (2001–2003, denoted as "current") and a future period (2051–2053, denoted as "future"). We prepared high-resolution initial and boundary meteorological conditions by running the WRF model at 12-km modeling domain driven by 6-hourly CCSM outputs with time-varying sea surface temperature and vegetation greenness fraction. Then, the outputs from 12-km runs were used as the inputs for the 4-km WRF/Chem model domain covering southeastern Texas and centered on the Houston metropolitan area. The simulations were performed for August of 2001–2003 and 2051–2053. To minimize the effect of initial conditions, the initial 2-day period (July 30 and July 31) of each simulation was considered as a spin-up period to establish the initial conditions for several atmospheric concentrations of different emission species.

2.3. Land Use and Land Cover Data

[11] The default land use and land cover data used in the WRF/Chem model are based on 1992–1993 USGS data and do not exactly reflect the land surface conditions of 2000s. We thus replaced this USGS data with the new data derived from 2000 Moderate Resolution Imaging Spectroradiometer (MODIS) data [*Friedl et al.*, 2002]. The 1-km MODIS land use and land cover types were classified by the International Geosphere-Biosphere Programme (IGBP), but excluded the permanent wetland and cropland and natural vegetation types. Three new classes of tundra and inland water bodies have been added by the Land Team at the National Centers for Environmental Prediction (NCEP) as an experimental product used here. Hence, there are 21 types of land use and land cover in the MODIS data set. A comparison of the USGS and MODIS data shows that land cover characteristics are different over the southeastern and surrounding areas of the Houston urban center. However, the dominant land cover types over these regions are relatively similar: "Dryland Cropland and Pasture" in the USGS data set, and "Cropland/Grassland Mosaic" in the MODIS data set. The largest difference occurs in the urban areas because of urban expansion. Moreover, to better characterize the present-day urban land use pattern, we incorporated high-resolution (30-m) USGS 2001 National Land Cover Database (NLCD) urban land use data with detailed urban land use classifications (low-intensity residential, high-intensity residential, and industrial or commercial) for the Houston area (Figure 1a).

[12] Future changes in land use patterns induced by human activities represent an important and highly uncertain control on near-surface meteorological conditions. We prepared the Houston urban land use data on the basis of future patterns of population density. The future patterns of population density were generated by the Spatially Explicit Regional Growth Model, which related population growth patterns with accessibility to urban and protected lands [*Theobald*, 2005]. The classification of different land use categories (high-density and low-density residential land use) needed for the UCM was processed according to the projected population density. We artificially treated the regions with population density larger than a certain value as the high-density residential areas. Low-density residential areas were characterized by a certain range of population density. As we did not have information about the future development of industrial-commercial areas, we kept the industrial-commercial land use the same as the current. We used the predicted urban land use distribution to the Houston urban area on the basis of the projected population growth to 2030. In 2030, the U.S. population is projected to grow 29%. We were limited to data projected to 2030, since projections to 2050 were unavailable. In fact, by 2050, if population continues to grow, the Houston urban area would expand, which may amplify the impacts of land use change. Although it is important to accurately represent all factors in the model, all model results are subject to uncertainty.

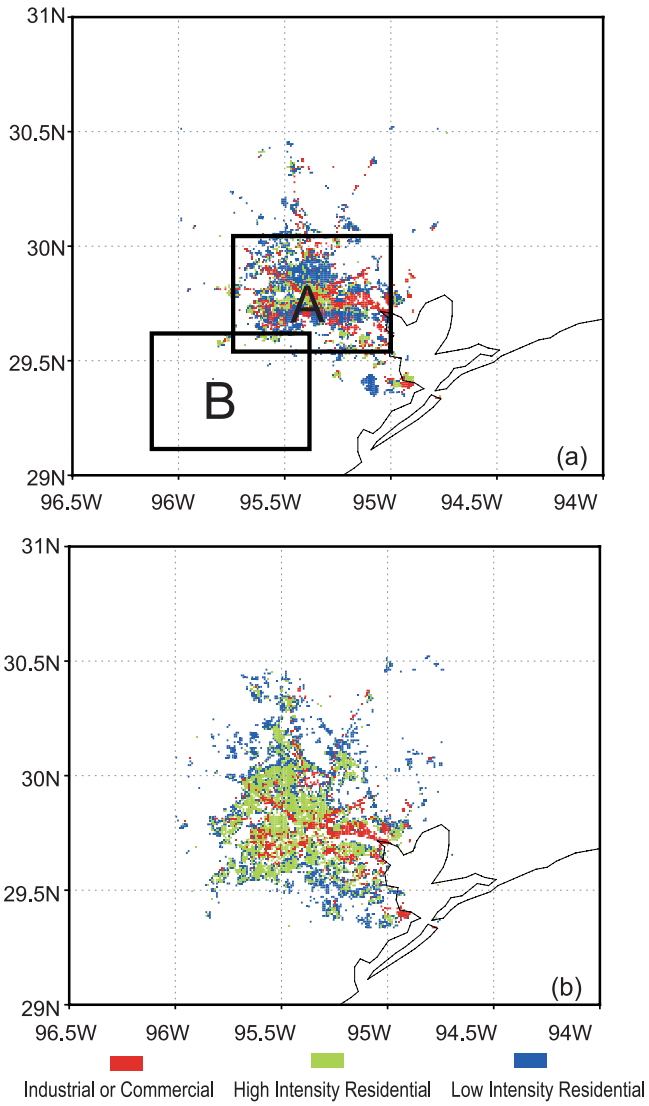

Figure 1. The three urban land use categories, industrial or commercial (red), high-intensity residential (light green), and low-intensity residential (blue), for (a) current years (2000s) defined from the NLCD database and a total area of urban land use of 3264 km^2 and (b) future years (2050s) defined on the basis of projected population growth in 2030 and a total urban land use area of 5293 km^2. Box A denotes the core urban area, and box B is for the suburban area.

Nevertheless, the future land use data used in our simulations at least provides us one possible scenario to study the impacts of future land use change on O_3. It should be noted that changes in land surface conditions in other regions are not considered in this study. Figures 1a and 1b show that urban land use area in the modeling domain increases almost by 62% in the future.

2.4. Anthropogenic and Biogenic Emissions

[13] Anthropogenic emissions of gas species for the years 2000 and 2050 are taken from the U.S. EPA's 1999 National Emissions Inventory (NEI-99, version 3) released in 2003 at a 4-km horizontal resolution (available from http://www.epa.gov/air/data/neidb.html). The emissions are representative of a typical summer day, as derived by temporal allocation factors specific to each source classification code provided by the EPA. This inventory is designed for regional-scale photochemical models of North America that require hourly emissions data for oxides of nitrogen (NO_x), volatile organic compounds (VOC), carbon monoxide (CO), sulfur dioxide (SO_2), and ammonia (NH_3). The emissions are speciated into 41 VOCs categories and are assigned a diurnal profile. The distribution of daily averaged nitrogen oxide (NO) emissions over the Houston area highlights the spatial correlation of the NO emissions and the urban land use (Figure 2a). In order to isolate effects of climate change and land use change from effects of anthropogenic emissions on surface O_3, the same anthropogenic emissions were applied for current and future year simulations. To examine the sensitivity of future change in surface O_3 to future changes in climate, land use, and anthropogenic emissions, future anthropogenic emissions are estimated by multiplying the present emissions by the growth factors for 2050s according to the SRES A1B scenario [*Wigley et al.*, 2002]. We multiplied CO, NO_x, VOC, and CH_4 by factors of 1.38, 1.55, 2.01, and 1.46, respectively, for the year 2053. A globally uniform CH_4 concentration for current year simulations is 1700 ppb and is projected to rise to 2480 ppb by 2050 in the A1B scenario. Concentrations of CO, NO_x and VOC, which are treated on the basis of NEI-99 for current years, are various across the modeling domain in the future scenario. Initial and boundary conditions for the gas-phase variables were based on those of *McKeen et al.* [2002], and the laterally invariant vertical profiles representing clean background were created from measurements collected onboard previous NASA-sponsored aircraft missions. Adjustments for boundary conditions are applied to the Houston area. In all simulations, the same chemical boundary conditions are used, which could give rise to some uncertainty in the model results.

[14] Biogenic emissions including isoprene, other biogenic volatile organic compounds (BVOCs), and NO, are very sensitive to changes in temperature and radiation. Emission rates of biogenic compounds at standard temperature and light conditions (Figure 2b) have been assigned to the model grid on the basis of the Biogenic Emissions Inventory System, version 3 (BEIS3), and the Biogenic Emissions Landuse Database, version 3 (BELD3), which provides distributions of 230 vegetation classes at 1-km resolution over North America [*Kinnee et al.*, 1997]. Then, biogenic emissions in all simulations are calculated online using the temperature and light-dependence algorithms from the BEIS3 [*Guenther et al.*, 1995; *Geron et al.*, 1994; *Williams et al.*, 1992].

2.5. Experiment Design

[15] To thoroughly evaluate the impacts, multiyear ensemble simulations would be preferred. However, to run multiyear simulations with this fully coupled atmosphere-chemistry model demands huge amounts of computing time. Under this circumstance, we carefully designed the experiments on the basis of a review of literature and examination of historical O_3 data over the Houston. Analysis of 20-year O_3 data shows that high O_3 episodes frequently occurred in August. Thus, an alternative way to

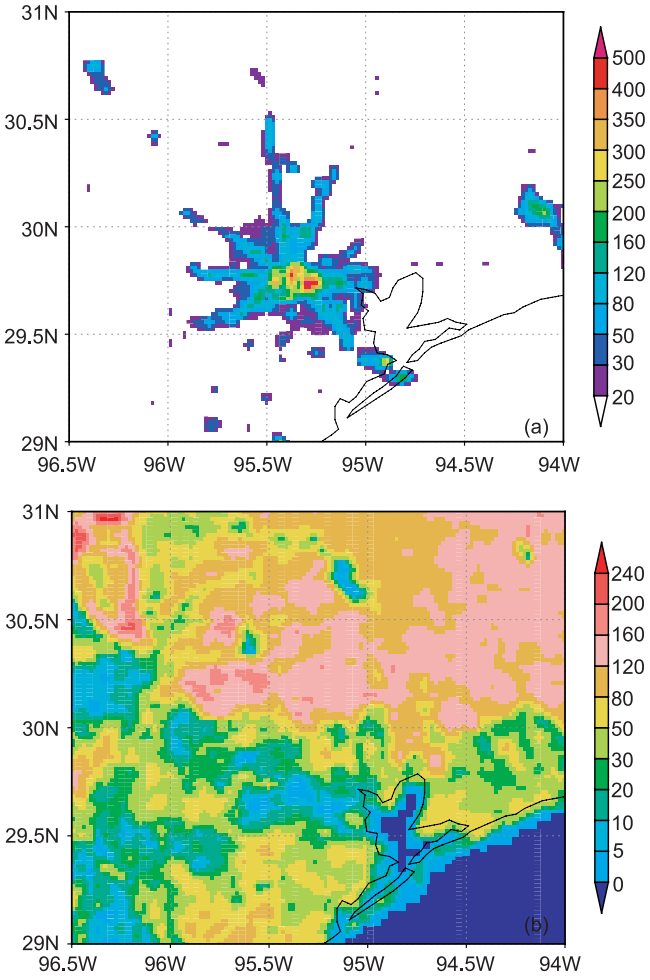

Figure 2. (a) Daily average anthropogenic NO emissions in summer (mol km^{-2} hr^{-1}) and (b) normalized biogenic emissions of isoprene generated by the BEIS3 (mol km^{-2} hr^{-1}). The normalized isoprene emissions are estimated at standard conditions of light, temperature, soil moisture, humidity, and leaf conditions, including a leaf area index of 5, a canopy with 92% mature leaves, a solar angle of 60°, a photosynthetic photon flux density transmission of 0.6, air temperature of 303 K, humidity at 14 g kg^{-1}, and soil moisture at 0.3 m^3 m^{-3}.

study the impacts on O_3 is to select August to represent summer season in order to avoid the limitation of computer resources. In previous studies of the impacts of anthropogenic emissions change and climate change on O_3 [*Hogrefe et al.*, 2004; *Liao et al.*, 2006; *Civerolo et al.*, 2007; *Tao et al.*, 2007], authors used either one summer season or five consecutive summer seasons for the present and future years to study the impacts. Thereby, we designed our experiments for three consecutive Augusts to represent the present and future scenarios respectively. In future studies, with increasingly available computational resources, multiyear runs would be the optimal way to assess the statistical significance of changes in O_3 caused by climate and land use change. Five experiments with different combinations of meteorological conditions, land use and anthropogenic emissions are listed in Table 2. The BASE simulation, which utilized current year land use data, climate conditions, and anthropogenic emissions, is used to assess the model performance and to calculate the predicted changes in the future. Simulations CL, CL-LU, CL-EMIS, and CL-EMIS-LU, with different combinations of future climate, land use, and future anthropogenic emissions, represent future year simulations. Simulations CL-EMIS and CL-EMIS-LU were carried out to understand the potential contribution of future change in anthropogenic emissions to O_3 formation in the Houston area in comparison with those of climate change and land use change.

3. Results and Discussion

3.1. Evaluation of Simulation Results for Current Year Conditions

[16] The success of the WRF/Chem model simulations was evaluated with a comparison of the model results with surface observations. Since our WRF/Chem simulations were driven by meteorological boundary conditions indirectly from a global climate simulation rather than a simulation of current weather, a direct comparison of the model output with hourly observations is not effective. Instead, the following analysis mainly focuses on an evaluation of the diurnal cycles of simulated monthly averaged daily temperature and O_3 concentrations and monthly averaged wind speed, which are very important to correctly simulating air quality sensitivity to climate change or land use change.

[17] *Dawson et al.* [2007] have examined the sensitivity of O_3 concentrations to summertime climate and found that temperature had the largest effect on air-quality standard exceedances, with a 2.5°C temperature increase leading to a 30% increase in the area exceeding the EPA standard. We evaluated the diurnal cycles of monthly averaged 2-m temperature and O_3 concentrations in 10 major sites maintained by the Texas Commission on Environmental Quality (TCEQ) over the Houston urban area (Figure 3). The data sets were downloaded from http://www.tceq.state.tx.us/compliance/monitoring/air/monops/historical_data.html. Figure 4a

Table 2. List of All Simulations[a]

Simulation	Simulation Period	Emissions	Land Use and Land Cover
Base	August 2001–2003	NEI-99 plus BEIS3	MODIS land cover plus NLCD land use
CL	August 2051–2053	NEI-99 plus BEIS3	MODIS land cover plus NLCD land use
CL-LU	August 2051–2053	NEI-99 plus BEIS3	MODIS land cover plus future land use
CL-EMIS	August 2053	future emissions plus BEIS 3	MODIS land cover plus NLCD land use
CL-LU-EMIS	August 2053	future emissions plus BEIS 3	MODIS land cover plus future land use

[a]NEI-99, U.S. EPA's 1999 National Emissions Inventory; BEIS3, Biogenic Emissions Inventory System, version 3; MODIS, Moderate Resolution Imaging Spectroradiometer; NLCD, National Land Cover Database.

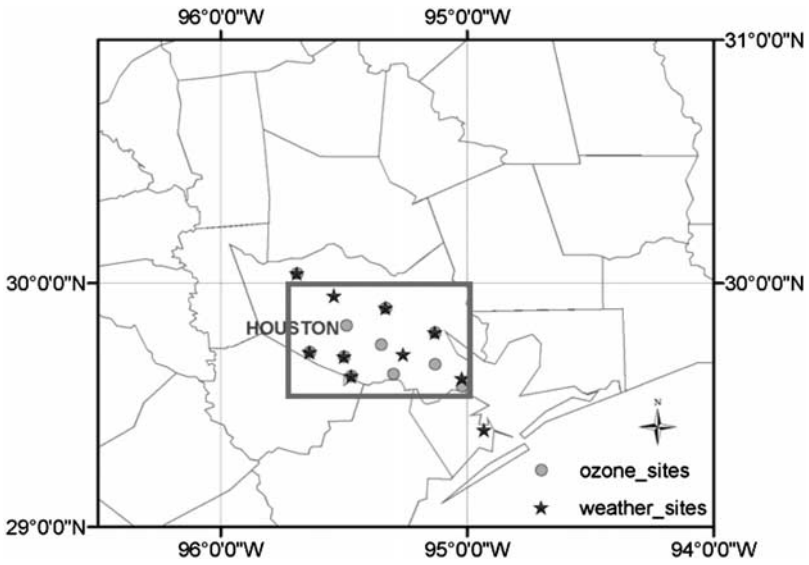

Figure 3. Map showing several surface observation stations used for model evaluation.

shows the diurnal evolutions of modeled and measured average 2-m temperature for August 2001–2003. The major pattern of simulated diurnal evolution of temperature is fairly similar to observations, especially during the daytime. The simulated higher nighttime temperature could be related to the uncertainties associated with parameters used in the UCM. As *Tokairin et al.* [2006] discussed in their work, the urban canopy model with the inclusion of buildings tends to overestimate nighttime temperature over the urban area. Thus, we speculate that the inappropriate building height parameters used in the UCM might lead to this overestimation. The agreement between simulations and measurements in the daytime O_3 concentrations is noteworthy (Figure 4b). However, the model clearly shows a distinct tendency to overpredict O_3 concentrations at night. This discrepancy is a common feature of other three-dimensional chemical transport models [*Lamb*, 1988; *Schere and Wayland*, 1989]. Several possible reasons are available to explain the high O_3 bias during the nighttime in the WRF/Chem model. Inaccuracies in the boundary layer dynamics could lead to higher O_3 concentrations. One possibility could be that the bottom model layer is too thick to allow efficient deposition at night. However, there are 30 vertical model layers, with finer vertical resolution in the lower troposphere to allow the model to simulate boundary layer processes more realistically. The bottom model layer is 17 m in all simulations. The depth of the bottom layer does not seem to be a reason causing higher nighttime O_3. After examining the model simulated NO, we found that the model tends to overpredict the OH concentration at low NO_x levels [*Eisele et al.*, 1994; *Mckeen et al.*, 1997], which can lead to a reduction in the destruction of O_3 at night. In the WRF/Chem simulations, the nighttime NO concentrations are very low, around 0.001 ppb. As a result, we do not focus on nighttime O_3 concentrations in our further analysis, but on the daytime and maximum 8-h O_3 concentrations.

[18] Comparison between the simulated and observed wind speeds (Figure 5) implies that the model has a relatively good performance in terms of simulating surface wind fields over the urban and surrounding regions. The average wind speed over the Houston urban center is around 1.8–2.1 m/s, which is quite close to observations. High wind speed in the south of the urban center is also well captured by the model. We also noticed that the model was able to capture the afternoon sea breeze over the Houston area as reflected by the wind rose pattern for the BASE simulation (as is seen later in Figure 7a). The evaluation of the model performance gives us confidence to examine the future air quality using this coupled model.

3.2. Regional Climate Change

[19] The occurrence of high O_3 concentrations during the summer is strongly determined by meteorological processes within the PBL. We briefly summarize the changes in the meteorological fields over the period between the 2000s and the 2050s on the basis of two simulations: CL-LU, which considers changes in both climate and land use, and BASE. In these simulations, anthropogenic emissions and chemical boundary conditions were fixed at the levels used for the current years, while the calculation of biogenic emissions took into account the effects of temperature and radiation changes under different climates. Meteorological conditions that are known to be associated with high O_3 concentrations are high mixing heights [*Rao et al.*, 2003], low wind speeds, and high temperatures [*Ordonez et al.*, 2005]. Here we discuss details of climate change, particularly those climate variables that are pertinent to O_3 chemistry.

[20] Modeling studies by *Sillman and Samson* [1995] and *Aw and Kleeman* [2003] have shown that summertime O_3 concentrations increase as temperature increases. Our model simulates a significant surface temperature rise between 2050s and 2000s. The highest increase in surface temperature during 12–18 LST occurs over the Houston urban area, as indicated by box A (here, we call it "zone A"), with an average increase of 3.3°C (Figure 6a). On average, the surface temperature is predicted to increase by about 2°C. This increase is also clearly apparent in CCSM3 outputs with an increase of 1.5°C in 2-m temperature in most parts of Texas. This is not unexpected, because incorporating a detailed UCM into the regional model at a high spatial

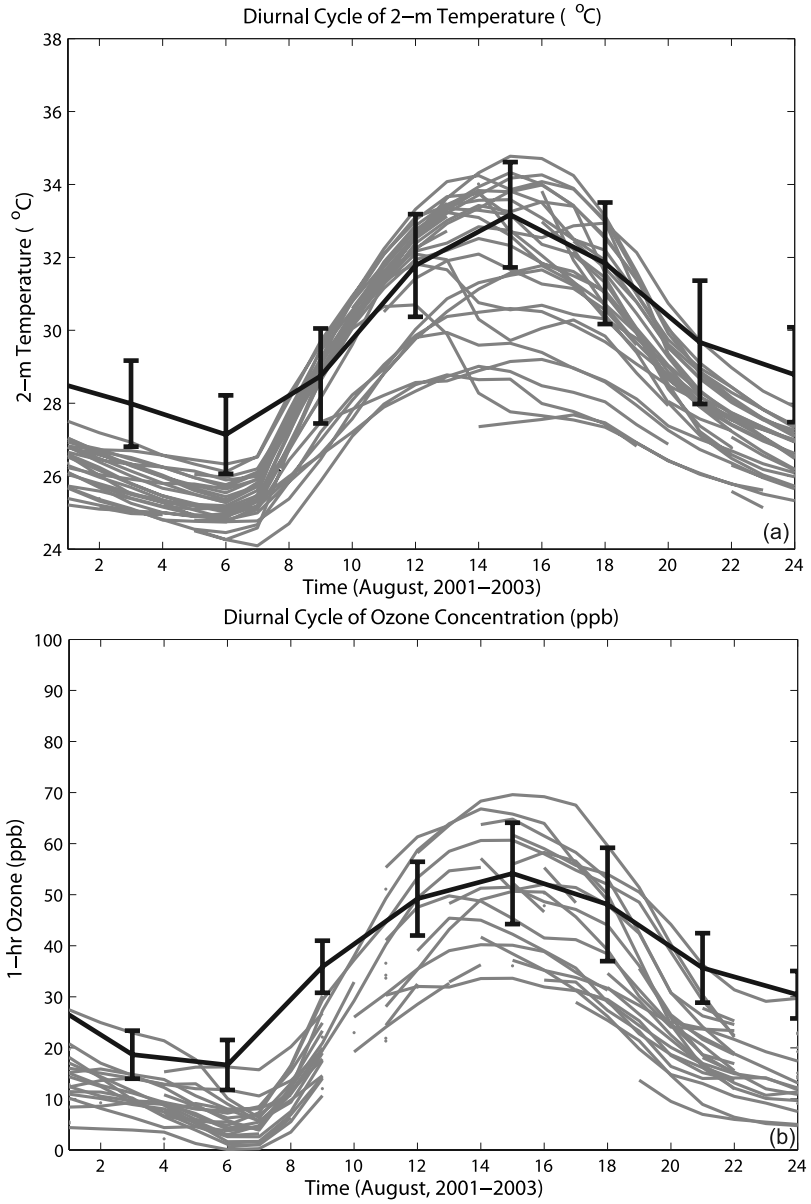

Figure 4. Observed and simulated (a) 2-m temperature and (b) O_3 concentrations during August 2001–2003. Gray lines represent the observations (the sites are shown in Figure 3), and black lines represent the simulated results for 31 days in August.

resolution can result in an increase in surface temperature which is somewhat higher than 2-m air temperature during the daytime. Figure 6b also shows that under projected future conditions considering changes in climate and land use, the Houston urban area tends to become drier. *Lin et al.* [2007] have shown that urban growth tends to decrease the relative humidity because of the increase in urban land surface which has less moisture than vegetated surfaces. Conversely, more water vapor coming from the warming ocean is responsible for higher water vapor mixing ratio along coastal regions. We also noticed that an increase in planetary boundary layer height (PBLH*)* occurs in the urban areas, with a maximum increase of 250 m and an average increase of 135 m (Figure 6c). As in the work of *Civerolo et al.* [2007], they suggest that extensive urban growth in the metropolitan area has the potential to increase afternoon near-surface temperature by 0.6°C and increase PBLH by more than 150 m. Here, the patterns in the differences of PBLH and surface temperature are identical. Moreover, under future climate conditions, we also see a daytime decrease in wind speeds with more reduction in the urban center (Figure 6d). The latter is attributed to the increase in roughness length associated with urbanization. The largest decrease of near-surface wind speeds is seen over the urban area (zone A) and southwest of the urban center as indicated by box B (here, we call it "zone B"). The wind direction also changes in response to changes in the distribution of temperature, relative humidity and surface roughness length. An evaluation of the wind rose patterns (Figure 7) indicates that the Houston area has more easterly winds in the afternoon because of future changes in climate and land use for the 2050s. It can be explained that as wind passes

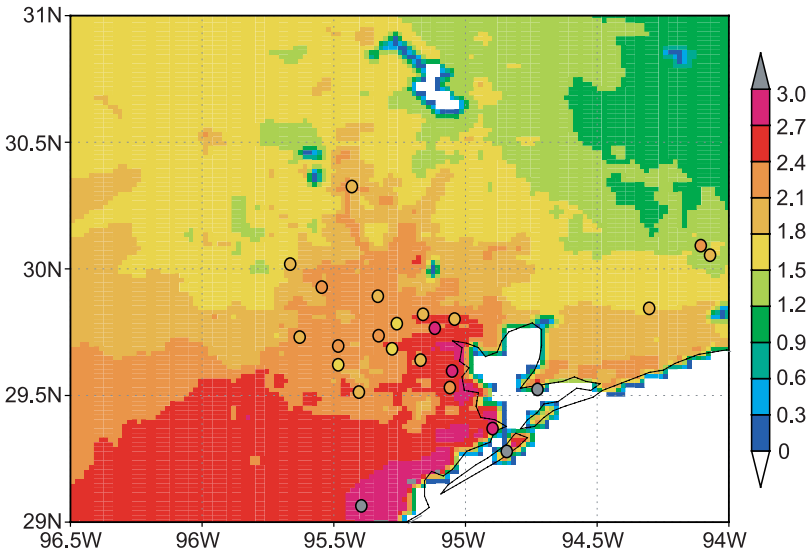

Figure 5. Observed (marked by circles) and simulated (shaded colors) wind speeds in Houston and surrounding areas.

through the urban area, the speed is slowed down because of high roughness length over the extended urban area. More urban land use leads to a decrease of near-surface wind speed in zone B. But it should be pointed out that there is no significant difference in wind speeds in the northwest and northeast of the modeling domain.

3.3. Impact on Regional Distribution of Photooxidants

[21] Future meteorological conditions observed in the simulations are favorable for O_3 formation. Increases in surface temperatures, reductions in wind speeds, and changes in boundary layer depths act to change O_3 levels through affecting the regional distribution of O_3 precursors such as NO_x and VOCs from anthropogenic and biogenic sources.

[22] Figure 8a displays the difference in simulated NO_x mixing ratios between the future and current years (assuming that anthropogenic emissions remain constant). A decrease in near-surface NO_x mixing ratios in the northern part of the Houston urban area and the northwest of the urban center can be attributed to increased PBLH. An increase in NO_x mixing ratio occurs over the southern part of the urban area and along the Bay area, associated with emission sources and decreased PBLH. The oxidation products of NO_x, such as nitric acid (HNO_3), are dependent on the NO_x concentrations. Figure 8b illustrates an increase in HNO_3 in the regions with high NO_x levels, and the highest increase of HNO_3 is mainly found along the Bay area and some parts of the urban area. The mixing ratio of peroxyacetyl nitrate (PAN) decreases in the northwest of the modeling domain (Figure 8c), which is mainly due to the increase in temperature that results in an enhanced thermal decomposition of PAN. Apart from the increased temperature, the presence of higher NO_x levels along coastal regions due to emission sources and reduced near-surface wind speeds as shown in Figure 6d favor PAN formation via chemical reactions.

[23] Carbonyl compounds can undergo photochemical reactions that will result in additional production of organic and hydrogen radicals, and produce more O_3. As seen in Figure 8d, over much of the modeling domain, formaldehyde (HCHO) increases as temperature increases in the future. This can be explained that the distribution of HCHO strongly depends on isoprene emissions, of which biogenic sources are predominant [*Wert et al.*, 2003]. Under future warm climate conditions, biogenic emissions are expected to increase. The model predicts a 20% increase in biogenic emissions of isoprene in response to future changes in temperature and radiation. It can be seen that the highest increase in HCHO concentrations mostly lies in rural regions, in particular, in the east of the Houston area, where the land surface is mostly covered by forests. Therefore, the significant increase in HCHO is expected to promote additional production of O_3 in the areas far from the urban center. However, it should be noted that future change in vegetation types is not considered in this study.

3.4. Changes in Surface O_3

[24] The analysis presented in section 3.3 implies that climate and land use change can cause significant changes in predicted concentrations of NO_x, HCHO, HNO_3, and PAN, which can further affect O_3 formation in the Houston area. Figure 9a depicts a spatial map of the difference in O_3 concentrations during the afternoon (1200 to 1800 LST) between the future and current year simulations. In the future year simulations, the anthropogenic emissions were fixed at the current level, while the urban land use change was considered (Table 2). For the 2050s, changes in summertime average daytime O_3 concentrations range from -2 to 8 ppb. The largest increases of 4–8 ppb are found over the surrounding regions of the urban center and zone B. However, O_3 concentrations are predicted to decrease in the northwest modeling domain. Analysis of model results suggests that this decrease is caused by the decreased water vapor mixing ratio, changed near-surface wind direction (discussed in section 3.2), and the low levels of NO_x. Because of more easterly winds in the future, fewer emissions are transported to northwest Houston area from the emission sources. The increased water vapor mixing ratio

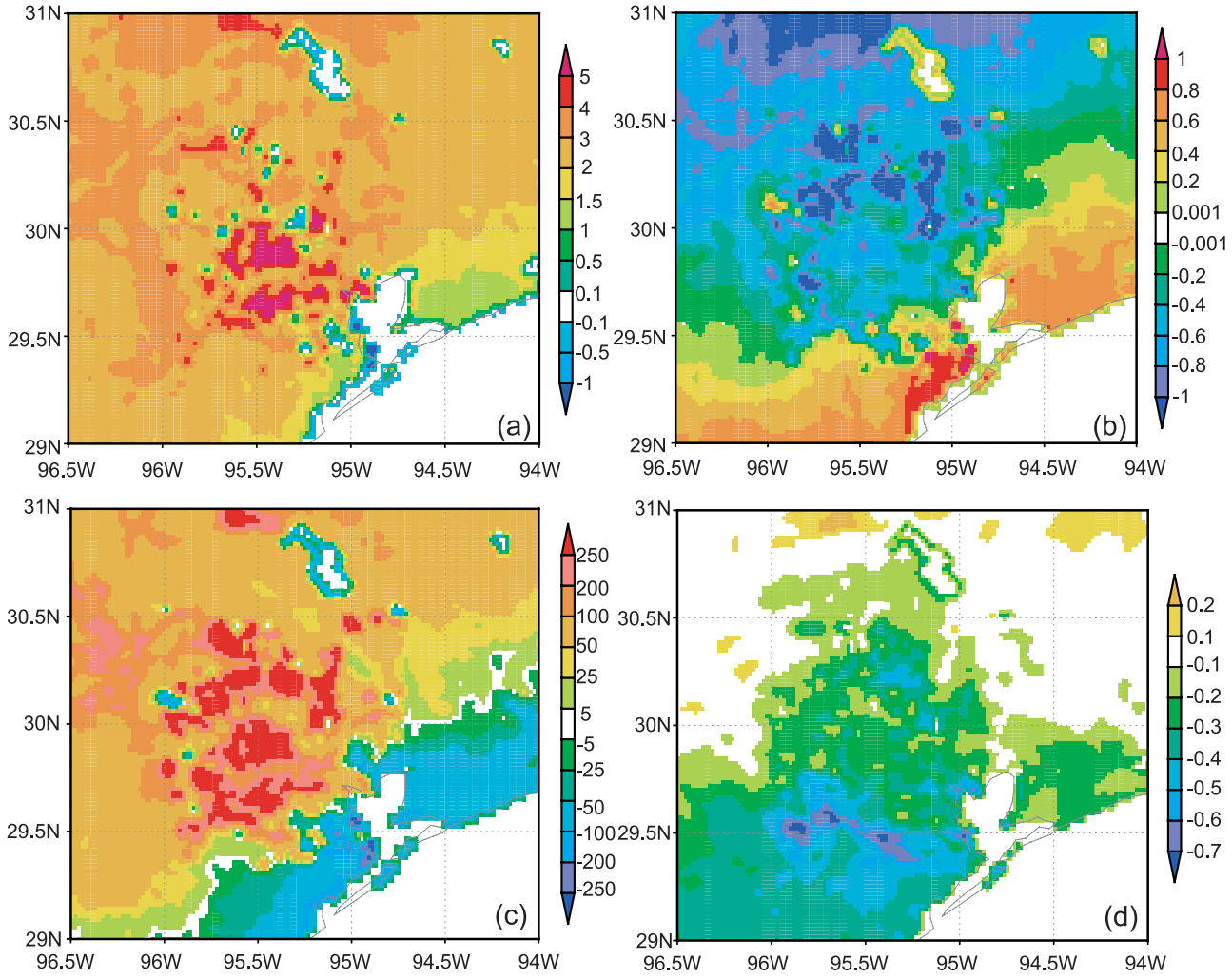

Figure 6. Simulated differences in afternoon (1200 to 1800 LST) (a) temperature (°C), (b) 2-m water vapor mixing ratio (k kg^{-1}), (c) planetary boundary layer height (PBLH) (m), and (d) 10-m wind speed (m s^{-1}) between CL-LU and BASE simulations for the month of August (ocean is masked out in all plots). CL-LU represents the future year simulations with the consideration of land use change, and BASE represents the present year simulations.

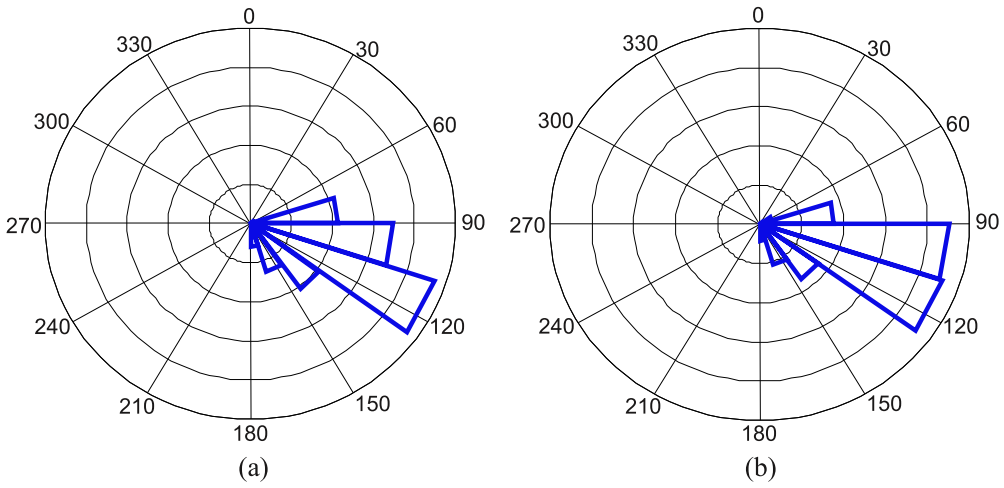

Figure 7. Simulated wind directions during the afternoon (1200 to 1800 LST) for (a) August 2001–2003 (BASE) and (b) August 2051–2053 (CL-LU).

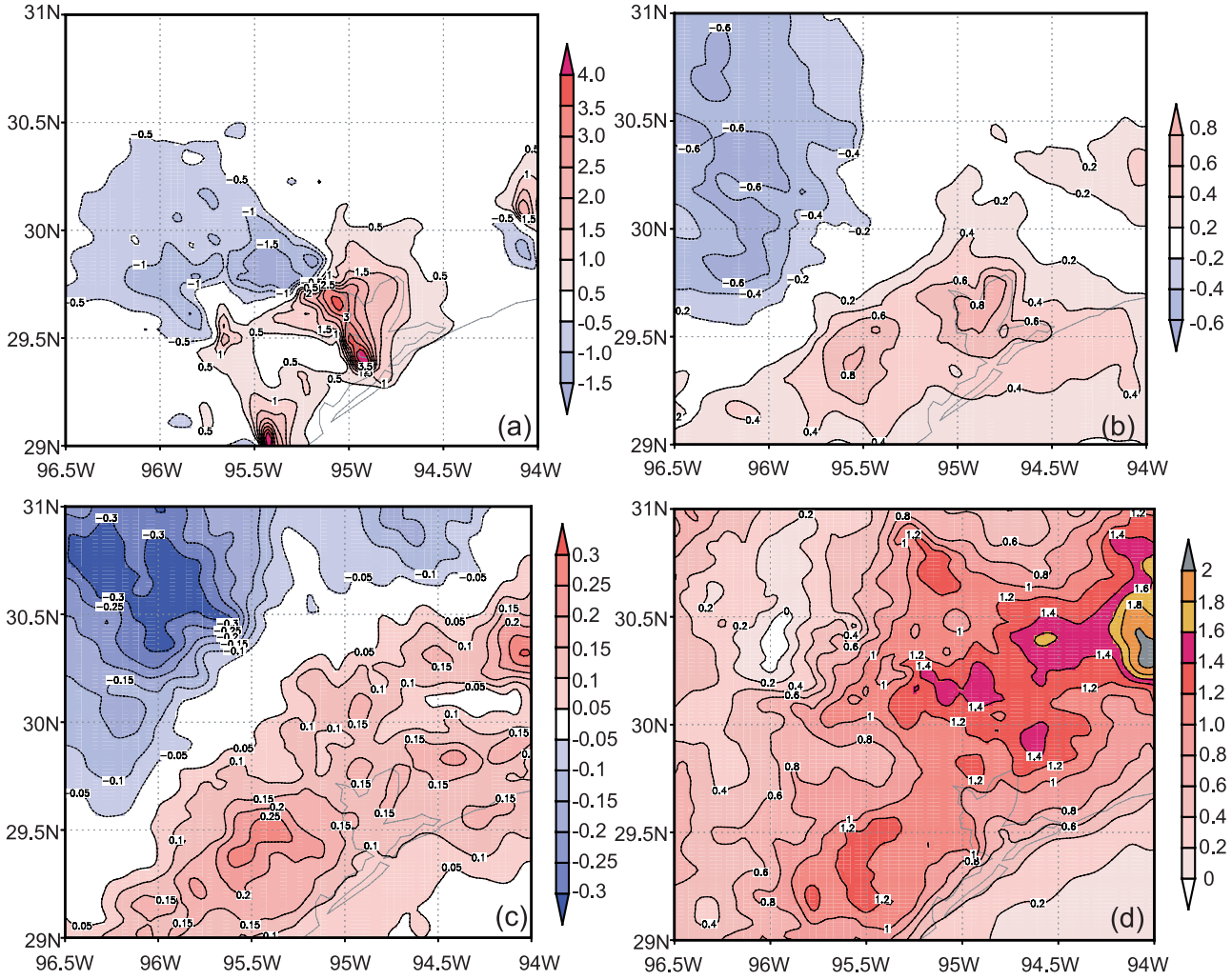

Figure 8. As in Figure 6 but for the differences in (a) NO_x, (b) HNO_3, (c) PAN, and (d) HCHO (ppb).

and decreased wind speeds along the coast, which is closer to the VOC and NO_x source regions, act to favor the formation of O_3. In the areas with high PAN levels, the O_3 concentrations are still high [*Singh et al.*, 1985]. We also find increasing isoprene emissions in response to future climate change tend to promote more O_3 formation in the modeling domain. In fact, this result is very sensitive to whether the reaction products of isoprene, isoprene nitrates,

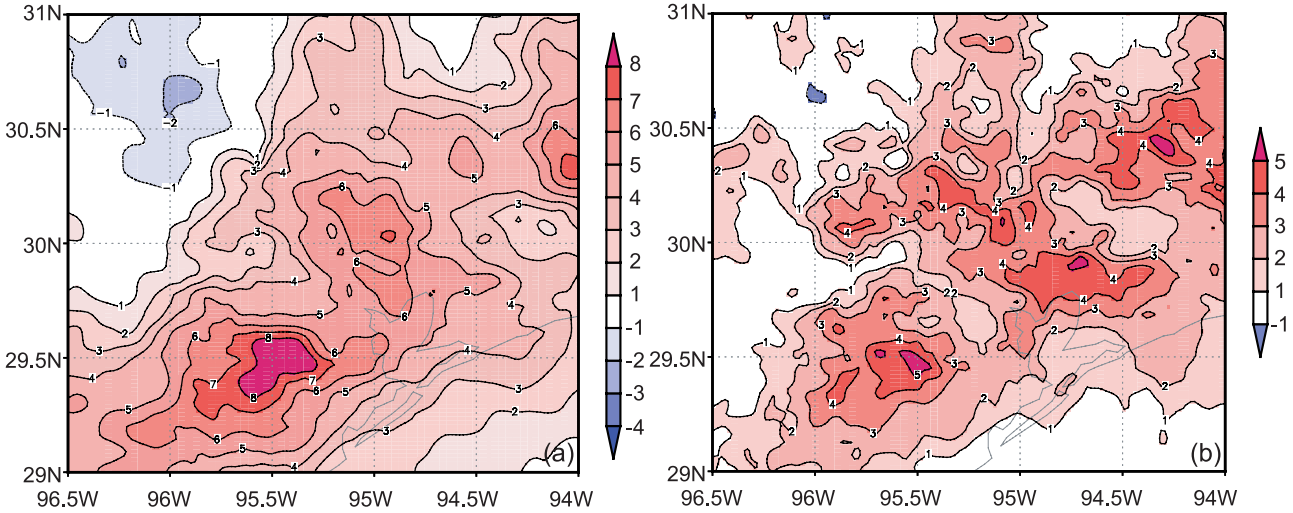

Figure 9. As in Figure 6 but for the differences in (a) O_3 concentrations (ppb) and (b) the number of days with the daily maximum 8-h O_3 concentrations larger than 84 ppb.

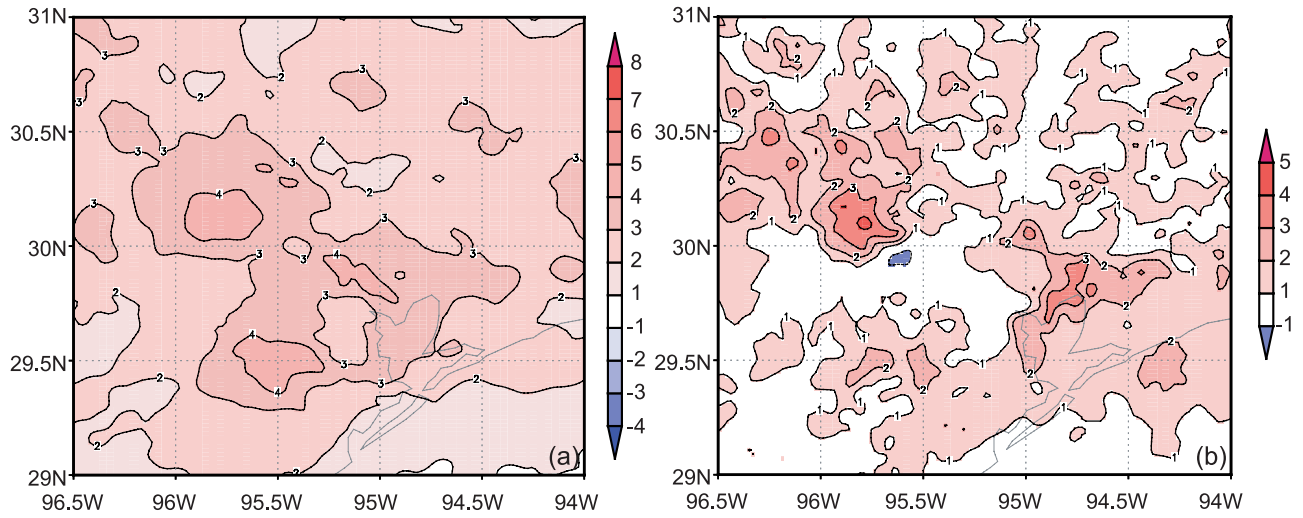

Figure 10. Simulated differences in (a) afternoon (1200 to 1800 LST) O_3 concentrations and (b) the number of days with the daily maximum 8-h O_3 concentrations larger than 84 ppb between CL-LU and CL simulations for the month of August. CL represents the future year simulations using the present year land use data.

represent a terminal or temporary sink for NO_x [*Horowitz et al.*, 2007]. *Wu et al.* [2008] found little climate-driven O_3 change in the southeastern United States, and they attributed this to the role isoprene nitrates play as a terminal sink for NO_x. In this study, we used the RADM2 chemical mechanism which only includes a very simple scheme of isoprene. Thus, the reaction products of isoprene, organic nitrates, are more likely to be a temporary sink for NO_x in our simulations.

[25] Because the U.S. NAAQS for 8-h O_3 concentration is set at 84 ppb, model-predicted exceedances of this threshold are of particular importance when assessing the effects of climate change and land use change on O_3 air quality. To analyze the changes in the frequency of predicted days with unhealthy O_3 concentrations (referred to as extreme O_3 days hereinafter), the number of days for which the predicted daily maximum 8-h O_3 concentrations exceeded 84 ppb was plotted in Figure 9b. The predicted distribution of the number of days with the maximum daily 8-h O_3 concentrations larger than 84 ppb matches the pattern of increased O_3 over the modeling domain. It can be seen that there is an increase of 4–5 days in the number of days with elevated O_3, with the largest increase over the surrounding regions of the urban center and zone B. Overall, the WRF/Chem simulations of O_3 concentrations utilizing the WRF downscaled 2050s A1B regional climate fields show an increase in summer average daily maximum 8-h O_3 concentrations and an increase in the number of extreme O_3 days over the Houston area due to future changes in climate and land use.

3.5. Contributions of Climate Change and Land Use Change to O_3 Changes

[26] Sensitivity simulations with the utilization of current and future land use data (CL and CL-LU) are used to discern the contribution of climate change and that of urban land use change to O_3 formation. Figure 10a shows that urban land use change promotes an increase of 1–4 ppb in average afternoon (1200 to 1800 LST) O_3 concentrations over much of the modeling domain in addition to climate change. Moreover, the higher O_3 caused by the land use change is associated with an increase of 1–3 days per month (August) in the number of extreme O_3 days (Figure 10b). The effects of land use change on both O_3 concentrations and extreme O_3 days are the most significant over the surrounding regions of the urban center, but not exactly over the urban center, which is consistent with *Civerolo et al.*'s [2007] results. In the core urban areas, NO_x emissions do not contribute to a significant increase in O_3 concentrations, but they do lead to increased O_3 formation in downwind areas. We attribute this increase in the spatial extent of VOC-limited regions to increasing urbanization. To be consistent with the future expansion of urban land use, the VOC-limited regions would be extended correspondingly.

[27] Figure 11 depicts the changes in average daily maximum 8-h O_3 concentrations due to climate change, land use change, and combined change. It can be seen that climate change alone causes −6–6 ppb change in O_3 (Figure 11a), and significant increases are found along the coast because of high NO_x emissions and warm temperatures. However, climate change alone does lead to a decrease in surface O_3 concentrations in areas further from the urban center (e.g., the northwest of the urban area or the rural areas). We ascribe this to the decreased water vapor mixing ratio and changed wind direction. When only considering the effects of future land use change (Figure 11b), a 2–6 ppb increase in daily maximum 8-h O_3 concentrations is found over much of the modeling domain with the largest increase located in the surrounding areas of the urban center. Furthermore, additional analysis indicates that land use change induces more O_3 formation over the areas (e.g., northwest of the domain) where climate change alone decreased O_3 concentrations. As the effects of both climate and land use changes are taken into account in the simu-

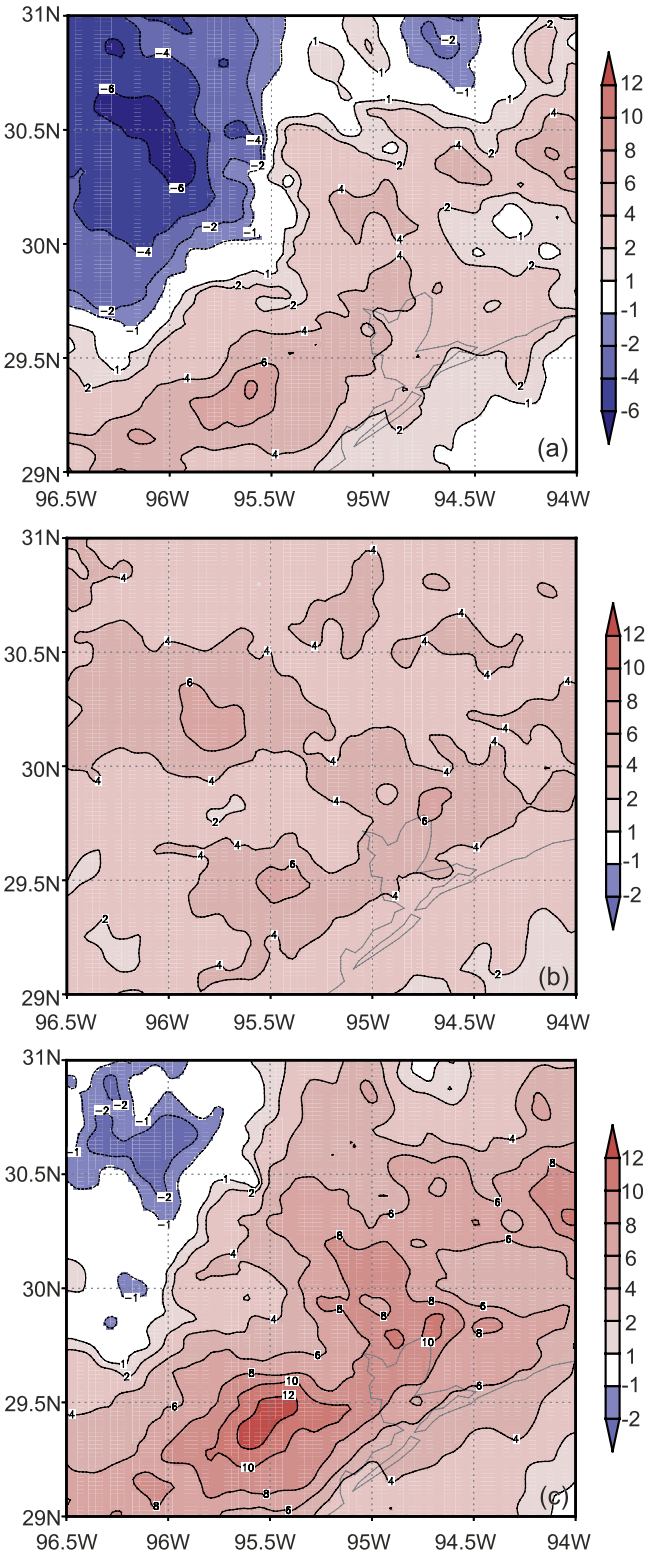

Figure 11. Changes in average daily maximum 8-h O_3 concentrations for (a) climate change effect (difference between CL and BASE simulations), (b) land use change effect (difference between CL-LU and CL simulations), and (c) combined climate change and land use change effect (difference between CL-LU and BASE simulations).

lations, daily maximum 8-h O_3 concentrations can increase up to 12 ppb in the 2050s (Figure 11c).

[28] We also plotted the frequency distributions of the simulated daily O_3 maxima during August over zones A and B. As we expected, because of the future changes in climate and land use, the frequency is shifted toward higher values (Figure 12). It seems that zone B is more likely to be affected by climate change, while zone A displays a pattern highly correlated with the land use change. Climate change alone leads to an increase in days with daily maximum 8-h O_3 at 65 ppb in zone B. This results in a significant increase of the number of days with near-surface O_3 concentrations higher than 84 ppb in this region, as was discussed above.

[29] The above analysis reveals that the impacts of climate change and land use change on O_3 differ across the modeling domain. The contributions of climate change and land use change are illustrated in a bar chart of changes in summertime average daily maximum 8-h O_3 concentrations for zones A and B (Figure 13). It can be seen that the effects of climate change alone account for an increase of 2.6 ppb in daily maximum 8-h O_3 concentrations in zone A. The land use change has more influence near the urban area than the climate change, with an additional increase of 1 ppb in daily maximum 8-h O_3 concentrations. The combined effects of climate and land use change on daily maximum 8-h O_3 concentrations can be up to 6.2 ppb. However, in zone B, which is more likely affected by the increased water vapor mixing ratio, reduced wind field and changed wind direction, and increased temperature, the impacts of climate change are stronger than those of future urban land use change.

[30] As discussed above, changes in meteorological variables have different impacts in different locations. To further quantify these impacts, a statistical correlation technique is applied to identify the contributions of different meteorological variables to O_3 formation due to climate change and land use change, respectively. A simple regression test was conducted and the correlation coefficients between O_3 concentration and these meteorological variables are summarized in Table 3. It is clear that near-surface temperature, wind speed, and humidity are very important meteorological factors influencing the variation in O_3 levels in the Houston area. We observed that temperature and water vapor mixing ratio have more influence on O_3 concentrations in zone B under future A1B climate scenario, notwithstanding the correlation between O_3 concentration and water vapor mixing ratio is negative. When the future land use change is considered in the simulations, the correlation between O_3 concentration and PBLH increases, indicating the important impact of land use change on the air quality over the urban areas. To a large extent, the correlation coefficients between temperature or water vapor mixing ratio and O_3 concentration are not affected in zone A. However, the coefficients are somewhat different in zone B. This further indicates that zone B is affected by meteorological variables to a larger degree than is zone A.

[31] The analysis above suggests that climate change and land use change have different impacts in different regions. Therefore, while many previous studies have pointed out the potentially important contribution of future climate

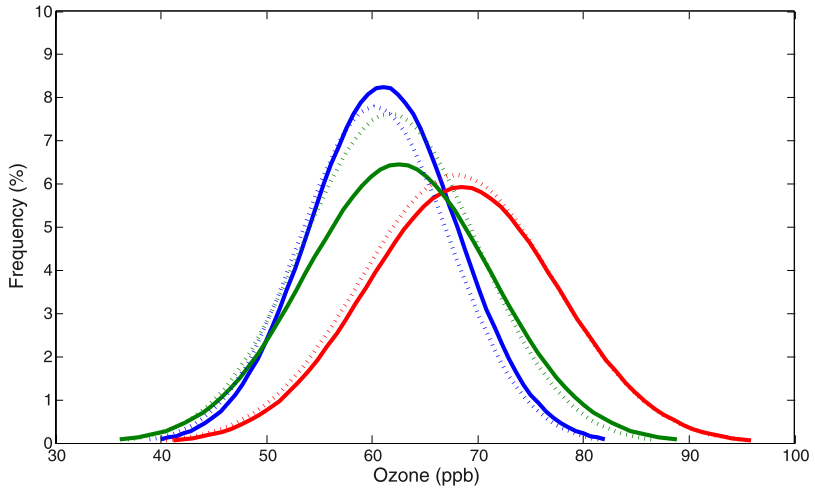

Figure 12. Frequency distributions of the simulated daily maximum 8-h O_3 concentrations averaged over zone A (dashed lines) and zone B (solid lines) during August for BASE (blue), CL (green), and CL-LU (red) simulations.

change and anthropogenic emissions to O_3 air quality for future decades, the results presented here imply that the effects of land use change may be at least equally important to the changing climate when planning for the future attainment of the NAAQS.

3.6. Sensitivity of Surface O_3 to Future Anthropogenic Emissions

[32] The analysis presented in the previous subsections focused on determining the effects of climate and land use change on summertime O_3 concentrations over the Houston area in the absence of changes in anthropogenic emissions within the modeling domain. Several studies have investigated the effects of increasing global and regional emissions on O_3 air quality using regional climate and air quality models [*Fiore et al.*, 2002, 2005; *Tagaris et al.*, 2007; *Tao et al.*, 2007]. It is of particular interest to compare the effects of climate and land use change to those caused by change in anthropogenic emissions. For brevity, we only did sensitivity simulations for the year 2053 using the current and future land use data (CL-EMIS and CL-LU-EMIS).

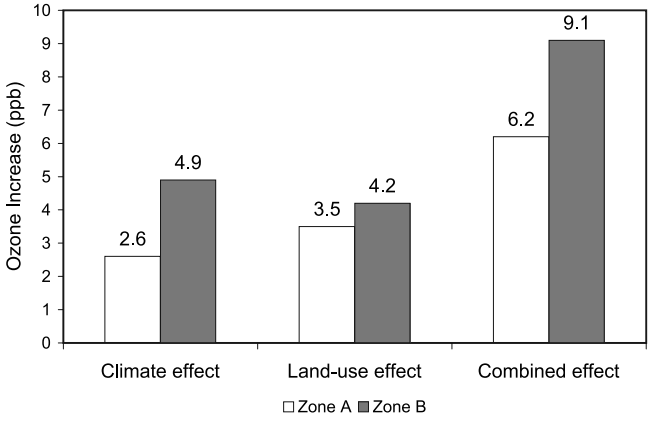

Figure 13. Spatially averaged contributions of climate-induced change, land use–induced change, and combined climate and land use change from the 2000s to the 2050s to changes in daily maximum 8-h O_3 concentrations.

[33] Figure 14 displays the percentage of the number of days in August with the daily maximum 8-h O_3 concentrations larger than 84 ppb over the Houston urban area. It can be seen that climate change induces around 8% increase in the extreme O_3 days over the urban area. When combined with the land use change, there is an additional 4% increase over the Houston urban area. There are more extreme O_3 days under future conditions with the consideration of climate and land use change in zone A than those in zone B. In zone B where the increased O_3 concentrations are relatively large, the increase in extreme O_3 days is not as significant as that in zone A. The anthropogenic emissions sensitivity experiment shows that the impacts of future change in anthropogenic emissions on extreme O_3 days are on the same order of those induced by climate and land use change. Still, zone A is affected more by changes in anthropogenic emissions than is zone B, since the former is a source area for anthropogenic emissions. Therefore the findings presented above may have potentially important implications for policy making concerning population health.

4. Conclusions

[34] This paper described the application of a coupled land-atmosphere-chemistry modeling system to understand

Table 3. Correlation Studies Between O_3 Concentrations and the Main Meteorological Variables

O_3	Zone	2-m Temperature	2-m Water Vapor Mixing Ratio	10-m Wind Speed	PBLH[a]
CL simulations	zone A	0.53	−0.63	−0.79	0.19
CL simulations	zone B	0.83	−0.89	−0.62	0.79
CL-LU simulations	zone A	0.51	−0.64	−0.60	0.59
CL-LU simulations	zone B	0.74	−0.92	−0.65	0.78

[a]Planetary boundary layer height.

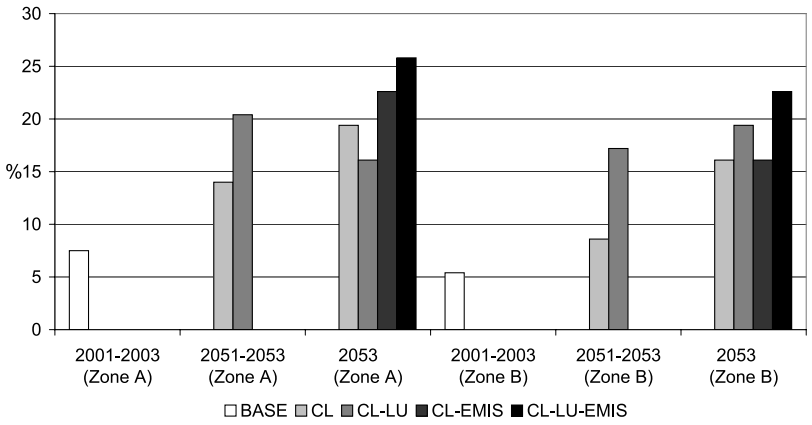

Figure 14. The percentage of the number of days with the daily maximum 8-h O_3 concentrations larger than 84 ppb over zone A and zone B. CL-LU-EMIS represents future year simulations with the consideration of future anthropogenic emissions change.

air quality in future decades over the Houston area. The effects on surface O_3 caused by future climate change under future A1B scenario and land use change are at least equally important in the Houston area. An increase in spatially and temporally average summertime daily maximum 8-h O_3 is found over most parts of the modeling domain, with a 6.2 ppb increase over the Houston area in the absence of changes in anthropogenic emissions. Climate change induces about an 8% increase in the extreme O_3 days and land use change adds an additional 6% increase over the Houston area. We also found that impacts of climate change and land use change on O_3 concentrations differ across the various areas of the domain. While the core urban area (zone A) is highly influenced by land use change, the suburban areas (e.g., zone B) are more likely affected by climate change. An increase in the number of extreme high O_3 days is found near the urban area, but not exactly in the urban center. This might be expected since O_3 is formed downwind of anthropogenic emission sources (except when weather is stagnant).

[35] Additional sensitivity simulations for the year 2053 investigating the relative impacts of changes in regional climate, anthropogenic emissions and land use on extreme O_3 days suggest that future anthropogenic emissions change also plays an important role as the climate and land use change does. In this study, we did not specifically address the effects of biogenic emissions on future changes in O_3 formation. It should also be pointed out here that the land use projections used in this study are relatively conservative, since they extend only as far as 2030, while the future climate conditions are from 2050. As both the population and the urban areas are expected to continue growing from 2030 to 2050, the urbanization impacts on O_3 are likely to be greater than reported in this study. Future studies that utilize a wide range of scenarios for climate, land use, and emissions to quantify the relative impacts of different factors on regional-scale air quality in a more comprehensive manner are needed.

[36] **Acknowledgments.** This work is supported by the U.S. EPA STAR program (grant RD83145201), the National Center for Atmospheric Research (NCAR) Advanced Study Program, the NCAR FY07 Director Opportunity Fund, and NASA Headquarters under the NASA Earth and Space Science Fellowship Program (grant NNX07AO28H). The NCAR is operated by the University Corporation for Atmospheric Research under sponsorship of the National Science Foundation. We are indebted to the land team at the NCEP for providing us the MODIS land cover data set and to Mukul Tewari for making the current land use data available to us. Shiguang Miao is thanked for helping set up the UCM in the WRF/Chem model. We thank Mary Barth, Xuexi Tie, Alex Guenther, Jerome Fast, William Vizuete, Gregory Frost, Steven Peckham, George Grell, Jonathan Pleim, Alma Hodzic, Peggy Lemone, and Susanne Grossman-Clarke for their valuable discussions during the course of this work. The computing resources are provided by the Texas Advanced Computing Center.

References

Aw, J., and M. J. Kleeman (2003), Evaluating the first-order effect of intraannual temperature variability on urban air pollution, *J. Geophys. Res.*, *108*(D12), 4365, doi:10.1029/2002JD002688.

Bossioli, E., M. Tombrou, A. Dandou, and N. Soulakellis (2007), Simulation of the effects of critical factors on ozone formation and accumulation in the greater Athens area, *J. Geophys. Res.*, *112*, D02309, doi:10.1029/2006JD007185.

Byun, D. W., et al. (2005), Estimation of biogenic emissions with satellite-derived land use and land cover data for air quality modeling of Houston-Galveston ozone nonattainment area, *J. Environ. Manage.*, *75*(4), 285–301, doi:10.1016/j.jenvman.2004.10.009.

Chen, F., and J. Dudhia (2001), Coupling an advanced land-surface/hydrology model with the Penn State/NCAR MM5 modeling system. Part I: Model description and implementation, *Mon. Weather Rev.*, *129*, 569–585, doi:10.1175/1520-0493(2001)129<0569:CAALSH>2.0.CO;2.

Chen, F., H. Kusaka, M. Tewari, J.-W. Bao, and H. Hirakuchi (2004), Utilizing the coupled WRF/LSM/Urban modeling system with detailed urban classification to simulate the urban heat island phenomena over the greater Houston area, paper presented at Fifth Conference on Urban Environment, Am. Meteorol. Soc., Vancouver, B. C., Canada.

Chen, F., M. Tewari, H. Kusaka, and T. T. Warner (2006), Current status of urban modeling in the community Weather Research and Forecast (WRF) model, paper presented at Sixth Symposium on the Urban Environment and AMS Forum: Managing our Physical and Natural Resources: Successes and Challenges, Am. Meteorol. Soc., Atlanta, Ga.

Civerolo, K. L., G. Sistla, S. T. Rao, and D. J. Nowak (2000), The effects of land use in meteorological modeling: Implications for assessment of future air quality scenarios, *Atmos. Environ.*, *34*(10), 1615–1621, doi:10.1016/S1352-2310(99)00393-3.

Civerolo, K. L., et al. (2007), Estimating the effects of increased urbanization on surface meteorology and ozone concentrations in the New York City metropolitan region, *Atmos. Environ.*, *41*, 1803–1818, doi:10.1016/j.atmosenv.2006.10.076.

Collins, W. D., et al. (2006), Radiative forcing by well-mixed greenhouse gases: Estimates from climate models in the Intergovernmental Panel on Climate Change (IPCC) Fourth Assessment Report (AR4), *J. Geophys. Res.*, *111*, D14317, doi:10.1029/2005JD006713.

Dabberdt, W. F., et al. (2004), Meteorological research needs for improved air quality forecasting: Report of the 11th Prospectus Development Team of the U.S. Weather Research Program, *Bull. Am. Meteorol. Soc.*, *85*(4), 563–586, doi:10.1175/BAMS-85-4-563.

Dawson, J. P., P. J. Adams, and S. N. Pandis (2007), Sensitivity of ozone to summertime climate in the eastern USA: A modeling case study, *Atmos. Environ.*, *41*, 1494–1511, doi:10.1016/j.atmosenv.2006.10.033.

Dudhia, J. (1989), Numerical study of convection observed during the winter monsoon experiment using a mesoscale two-dimensional model, *J. Atmos. Sci.*, *46*, 3077–3107, doi:10.1175/1520-0469(1989)046<3077:NSOCOD>2.0.CO;2.

Eisele, F. L., G. H. Mount, F. C. Fehsenfeld, J. Harder, E. Marovich, D. D. Parrish, J. Roberts, M. Trainer, and D. Tanner (1994), Intercomparison of tropospheric OH and ancillary trace gas measurements at Fritz Peak Observatory, Colorado, *J. Geophys. Res.*, *99*(D9), 18,605–18,626, doi:10.1029/94JD00740.

Ek, M. B., K. E. Mitchell, Y. Lin, E. Rogers, P. Grunmann, V. Koren, G. Gayno, and J. D. Tarpley (2003), Implementation of Noah land surface model advances in the National Centers for Environmental Prediction operational mesoscale Eta model, *J. Geophys. Res.*, *108*(D22), 8851, doi:10.1029/2002JD003296.

Fast, J. D., and W. E. Heilman (2005), Simulated sensitivity of seasonal ozone exposure in the Great Lakes region to changes in anthropogenic emissions in the presence of interannual variability, *Atmos. Environ.*, *39*(29), 5291–5306, doi:10.1016/j.atmosenv.2005.05.032.

Fast, J. D., W. I. Gustafson Jr., R. C. Easter, R. A. Zaveri, J. C. Barnard, E. G. Chapman, G. A. Grell, and S. E. Peckham (2006), Evolution of ozone, particulates, and aerosol direct radiative forcing in the vicinity of Houston using a fully coupled meteorology-chemistry-aerosol model, *J. Geophys. Res.*, *111*, D21305, doi:10.1029/2005JD006721.

Fiore, A. M., D. J. Jacob, I. Bey, R. M. Yantosca, B. D. Field, A. C. Fusco, and J. G. Wilkinson (2002), Background ozone over the United States in summer: Origin, trend, and contribution to pollution episodes, *J. Geophys. Res.*, *107*(D15), 4275, doi:10.1029/2001JD000982.

Fiore, A. M., et al. (2005), Evaluating the contribution of changes in isoprene emissions to surface ozone trends over the eastern United States, *J. Geophys. Res.*, *110*, D12303, doi:10.1029/2004JD005485.

Forkel, R., and R. Knoche (2006), Regional climate change and its impact on photooxidant concentrations in southern Germany: Simulations with a coupled regional climate-chemistry model, *J. Geophys. Res.*, *111*, D12302, doi:10.1029/2005JD006748.

Friedl, M. A., et al. (2002), Global land cover mapping from MODIS: Algorithms and early results, *Remote Sens. Environ.*, *83*, 287–302, doi:10.1016/S0034-4257(02)00078-0.

Geron, C. D., A. B. Guenther, and T. E. Pierce (1994), An improved model for estimating emissions of volatile organic compounds from forests in the eastern United States, *J. Geophys. Res.*, *99*(D6), 12,773–12,792, doi:10.1029/94JD00246.

Grell, G. A., J. Dudhia, and D. R. Stauffer (1994), A description of the fifth-generation Penn State/NCAR mesoscale model (MM5), *NCAR Tech. Note NCAR/TN-398+STR*, 117 pp., Natl. Cent. Atmos. Res., Boulder, Colo.

Grell, G. A., S. E. Peckham, R. Schmitzc, S. A. McKeenb, G. Frostb, W. C. Skamarockd, and B. Eder (2005), Fully coupled "online" chemistry within the WRF model, *Atmos. Environ.*, *39*, 6957–6975, doi:10.1016/j.atmosenv.2005.04.027.

Grossman-Clarke, S., et al. (2005), Urban modifications in a mesoscale meteorological model and the effects on near-surface variables in an arid metropolitan region, *J. Appl. Meteorol.*, *44*(9), 1281–1297, doi:10.1175/JAM2286.1.

Guenther, A., et al. (1995), A global model of natural volatile organic compound emissions, *J. Geophys. Res.*, *100*(D5), 8873–8892, doi:10.1029/94JD02950.

Hogrefe, C., B. Lynn, K. Civerolo, J.-Y. Ku, J. Rosenthal, C. Rosenzweig, R. Goldberg, S. Gaffin, K. Knowlton, and P. L. Kinney (2004), Simulating changes in regional air pollution over the eastern United States due to changes in global and regional climate and emissions, *J. Geophys. Res.*, *109*, D22301, doi:10.1029/2004JD004690.

Holt, T., and J. Pullen (2007), Urban canopy modeling of the New York City metropolitan area: A comparison and validation of single- and multilayer parameterizations, *Mon. Weather Rev.*, *135*(5), 1906–1930, doi:10.1175/MWR3372.1.

Hong, S. Y., and H. L. Pan (1996), Nonlocal boundary layer vertical diffusion in a medium range forecast model, *Mon. Weather Rev.*, *124*, 2322–2339, doi:10.1175/1520-0493(1996)124<2322:NBLVDI>2.0.CO;2.

Hong, S.-Y., J. Dudhia, and S.-H. Chen (2004), A revised approach to ice microphysical processes for the bulk parameterization of clouds and precipitation, *Mon. Weather Rev.*, *132*, 103–120, doi:10.1175/1520-0493(2004)132<0103:ARATIM>2.0.CO;2.

Horowitz, L. W., A. M. Fiore, G. P. Milly, R. C. Cohen, A. Perring, P. J. Wooldridge, P. G. Hess, L. K. Emmons, and J.-F. Lamarque (2007), Observational constraints on the chemistry of isoprene nitrates over the eastern United States, *J. Geophys. Res.*, *112*, D12S08, doi:10.1029/2006JD007747.

Inoue, E. (1963), On the turbulent structure of air flow within crop canopies, *J. Met. Soc. Jpn.*, *41*(6), 317–326.

Intergovernmental Panel on Climate Change (IPCC) (2001), *Climate Change 2001:The Scientific Basis—Contribution of Working Group I to the Third Assessment Report of the Intergovernmental Panel on Climate Change*, edited by J. T. Houghton et al., 881 pp., Cambridge Univ. Press, New York.

Intergovernmental Panel on Climate Change (IPCC) (2007), *Climate Change 2007: The Scientific Basis—Contribution of Working Group I to the Fourth Assessment Report of the Intergovernmental Panel on Climate Change*, edited by S. Solomon et al., Cambridge Univ. Press, New York.

Jiang, G. F., and J. D. Fast (2004), Modeling the effects of VOC and NO_X emission sources on ozone formation in Houston during the TexAQS 2000 field campaign, *Atmos. Environ.*, *38*(30), 5071–5085, doi:10.1016/j.atmosenv.2004.06.012.

Jimenez, P., et al. (2006), Evaluation of MM5-EMICAT2000-CMAQ performance and sensitivity in complex terrain: High-resolution application to the northeastern Iberian Peninsula, *Atmos. Environ.*, *40*(26), 5056–5072, doi:10.1016/j.atmosenv.2005.12.060.

Kinnee, E., C. Geron, and T. Pierce (1997), United States land use inventory for estimation biogenic ozone precursor emissions, *Ecol. Appl.*, *7*, 46–58, doi:10.1890/1051-0761(1997)007[0046:USLUIF]2.0.CO;2.

Kusaka, H., and F. Kimura (2004a), Thermal effects of urban canyon structure on the nocturnal heat island: Numerical experiment using a mesoscale model coupled with an urban canopy model, *J. Appl. Meteorol.*, *43*, 1899–1910, doi:10.1175/JAM2169.1.

Kusaka, H., and F. Kimura (2004b), Coupling a single-layer urban canopy model with a simple atmospheric model: Impact of urban heat island simulation for an idealized case, *J. Meteorol. Soc. Jpn.*, *82*, 67–80, doi:10.2151/jmsj.82.67.

Kusaka, H., H. Kondo, Y. Kikegawa, and F. Kimura (2001), A simple single-layer urban canopy model for atmospheric models: Comparison with multi-layer and slab models, *Boundary Layer Meteorol.*, *101*, 329–358, doi:10.1023/A:1019207923078.

Lamb, R. G. (1988), Diagnostic studies of ozone in the northeastern United States based on application of the Regional Oxidant Model (ROM), in *The Scientific and Technical Issues Facing Post–1987 Ozone Control Strategies*, edited by G. T. Wolff, J. L. Hanisch, and K. Schere, Air Waste Manage. Assoc., Pittsburgh, Pa.

Leung, L. R., and W. I. Gustafson Jr. (2005), Potential regional climate change and implications to U.S. air quality, *Geophys. Res. Lett.*, *32*, L16711, doi:10.1029/2005GL022911.

Li, G., R. Zhang, J. Fan, and X. Tie (2007), Impacts of biogenic emissions on photochemical ozone production in Houston, Texas, *J. Geophys. Res.*, *112*, D10309, doi:10.1029/2006JD007924.

Liao, H., W.-T. Chen, and J. H. Seinfeld (2006), Role of climate change in global predictions of future tropospheric ozone and aerosol, *J. Geophys. Res.*, *111*, D12304, doi:10.1029/2005JD006852.

Lin, W. S., et al. (2007), A numerical study of the influence of urban expansion on monthly climate in dry autumn over the Pearl River Delta, China, *Theor. Appl. Climatol.*, *89*(1–2), 63–72, doi:10.1007/s00704-006-0244-6.

Liu, Y., F. Chen, T. Warner, and J. Basara (2006), Verification of a mesoscale data-assimilation and forecasting system for the Oklahoma City area during the Joint Urban 2003 field project, *J. Appl. Meteorol. Climatol.*, *45*, 912–929, doi:10.1175/JAM2383.1.

Lo, J. C. F., A. K. H. Lau, F. Chen, J. C. H. Fung, and K. K. M. Leung (2007), Urban modification in a mesoscale model and the effects on the local circulation in the Pearl River Delta region, *J. Appl. Meteorol. Climatol.*, *46*, 457–476, doi:10.1175/JAM2477.1.

Madronich, S. (1987), Photodissociation in the atmosphere: I. Actinic flux and the effects of ground reflections and clouds, *J. Geophys. Res.*, *92*, 9740–9752, doi:10.1029/JD092iD08p09740.

Martin, R. V., D. J. Jacob, R. M. Yantosca, M. Chin, and P. Ginoux (2003), Global and regional decreases in tropospheric oxidants from photochemical effects of aerosols, *J. Geophys. Res.*, *108*(D3), 4097, doi:10.1029/2002JD002622.

McKeen, S. A., et al. (1997), Photochemical modeling of hydroxyl and its relationship to other species during the Tropospheric OH Photochemistry Experiment, *J. Geophys. Res.*, *102*(D5), 6467–6494, doi:10.1029/96JD03322.

McKeen, S. A., et al. (2002), Ozone production from Canadian wildfires during June and July of 1995, *J. Geophys. Res.*, *107*(D14), 4192, doi:10.1029/2001JD000697.

Meehl, G. A., et al. (2006), Climate change projections for the twenty-first century and climate change commitment in the CCSM3, *J. Clim.*, *19*(11), 2597–2616, doi:10.1175/JCLI3746.1.

Mickley, L. J., D. J. Jacob, B. D. Field, and D. Rind (2004), Effects of future climate change on regional air pollution episodes in the United States, *Geophys. Res. Lett.*, *31*, L24103, doi:10.1029/2004GL021216.

Mlawer, E. J., S. J. Taubman, P. D. Brown, M. J. Iacono, and S. A. Clough (1997), Radiative transfer for inhomogeneous atmospheres: RRTM, a validated correlated-k model for the longwave, *J. Geophys. Res.*, *102*(D14), 16,663–16,682, doi:10.1029/97JD00237.

Murazaki, K., and P. Hess (2006), How does climate change contribute to surface ozone change over the United States?, *J. Geophys. Res.*, *111*, D05301, doi:10.1029/2005JD005873.

Nam, J., Y. Kimura, W. Vizuete, C. Murphy, and D. T. Allen (2006), Modeling the impacts of emission events on ozone formation in Houston, Texas, *Atmos. Environ.*, *40*, 5329–5341, doi:10.1016/j.atmosenv.2006.05.002.

Ordonez, C., H. Methis, M. Furger, S. Henne, C. Huglin, J. Staehelin, and A. S. H. Prevot (2005), Changes of daily surface ozone maxima in Switzerland in all seasons from 1992 to 2002 and discussion of summer 2003, *Atmos. Chem. Phys.*, *5*, 1187–1203.

Prather, M., et al. (2003), Fresh air in the 21st century?, *Geophys. Res. Lett.*, *30*(2), 1100, doi:10.1029/2002GL016285.

Racherla, P. N., and P. J. Adams (2006), Sensitivity of global tropospheric ozone and fine particulate matter concentrations to climate change, *J. Geophys. Res.*, *111*, D24103, doi:10.1029/2005JD006939.

Rao, S. T., J. Y. Ku, S. Berman, D. Zhang, and H. Mao (2003), Summertime characteristics of the atmospheric boundary layer and relationships to ozone levels over the eastern United States, *Pure Appl. Geophys.*, *160*, 21–55, doi:10.1007/s00024-003-8764-9.

Schere, K. L., and R. A. Wayland (1989), EPA Regional Oxidant Model (ROM2.0): Evaluation on 1980 NEROS Data Bases, *Rep. EPA–600/3–89/057*, Research Triangle Park, N. C.

Sillman, S., and P. J. Samson (1995), Impact of temperature on oxidant photochemistry in urban, polluted rural and remote environments, *J. Geophys. Res.*, *100*(D6), 11,497–11,508, doi:10.1029/94JD02146.

Singh, H. B., et al. (1985), Relationship between peroxyacetyl nitrate and nitrogen oxides in the clean troposphere, *Nature*, *318*, 347–349, doi:10.1038/318347a0.

Skamarock, W. C., J. B. Klemp, J. Dudhia, D. O. Gill, D. M. Barker, W. Wang, and J. D. Powers (2005), A description of the Advanced Research WRF version 2, *Tech. Rep. TN-468+STR*, 88 pp., Natl. Cent. Atmos. Res., Boulder, Colo.

Stockwell, W. R., P. Middleton, J. S. Chang, and X. Tang (1990), The second generation regional acid deposition model chemical mechanism for regional air quality modeling, *J. Geophys. Res.*, *95*(D10), 16,343–16,367, doi:10.1029/JD095iD10p16343.

Taha, H. (1996), Modeling the impacts of increased urban vegetation on the ozone air quality in the South Coast Air Basin, *Atmos. Environ.*, *30*(20), 3423–3430, doi:10.1016/1352-2310(96)00035-0.

Taha, H., S. Konopacki, and H. Akbari (1998), Impacts of lowered urban air temperatures on precursor emission and ozone air quality, *J. Air Waste Manage. Assoc.*, *48*, 860–865.

Tao, Z., A. Williams, H.-C. Huang, M. Caughey, and X.-Z. Liang (2007), Sensitivity of U.S. surface ozone to future emissions and climate changes, *Geophys. Res. Lett.*, *34*, L08811, doi:10.1029/2007GL029455.

Tao, Z. N., et al. (2004), Sensitivity of regional ozone concentrations to temporal distribution of emissions, *Atmos. Environ.*, *38*(37), 6279–6285, doi:10.1016/j.atmosenv.2004.08.042.

Tie, X., G. Brasseur, L. Emmons, L. Horowitz, and D. Kinnison (2001), Effects of aerosols on tropospheric oxidants: A global model study, *J. Geophys. Res.*, *106*(D19), 22,931–22,964, doi:10.1029/2001JD900206.

Theobald, D. (2005), Landscape patterns of exurban growth in the USA from 1980 to 2020, *Ecol. Soc.*, *10*(1), 32.

Tokairin, T., H. Kondo, H. Yoshikado, Y. Genchi, and T. Ihara (2006), Numerical study on the effect of buildings on temperature variation in urban and suburban areas in Tokyo, *J. Meteorol. Soc. Jpn.*, *84*(5), 921–937, doi:10.2151/jmsj.84.921.

Wang, X. M., W. S. Lin, L. M. Yang, R. R. Deng, and H. Lin (2007), A numerical study of influences of urban land use change on ozone distribution over the Pearl River Delta region, China, *Tellus, Ser. B*, *59*(3), 633–641, doi:10.1111/j.1600-0889.2007.00271.x.

Weng, Q., et al. (2006), Urban air pollution patterns, land use, and thermal landscape: An examination of the linkage using GIS, *Environ. Monit. Assess.*, *117*(1–3), 463–489, doi:10.1007/s10661-006-0888-9.

Wert, B. P., et al. (2003), Signatures of terminal alkene oxidation in airborne formaldehyde measurements during TexAQS 2000, *J. Geophys. Res.*, *108*(D3), 4104, doi:10.1029/2002JD002502.

Wigley, T. M. L., S. J. Smith, and M. J. Prather (2002), Radiative forcing due to reactive gas emissions, *J. Clim.*, *15*(18), 2690–2696, doi:10.1175/1520-0442(2002)015<2690:RFDTRG>2.0.CO;2.

Williams, E. J., A. Guenther, and F. C. Fehsenfeld (1992), An inventory of nitric oxide emissions from solids in the United States, *J. Geophys. Res.*, *97*(D7), 7511–7519.

Wu, S., L. J. Mickley, E. M. Leibensperger, D. J. Jacob, D. Rind, and D. G. Streets (2008), Effects of 2000–2050 global change on ozone air quality in the United States, *J. Geophys. Res.*, *113*, D06302, doi:10.1029/2007JD008917.

Zhang, F., N. Bei, J. W. Nielsen-Gammon, G. Li, R. Zhang, A. Stuart, and A. Aksoy (2007), Impacts of meteorological uncertainties on ozone pollution predictability estimated through meteorological and photochemical ensemble forecasts, *J. Geophys. Res.*, *112*, D04304, doi:10.1029/2006JD007429.

F. Chen and C. Wiedinmyer, National Center for Atmospheric Research, P.O. Box 3000, Boulder, CO 80307-3000, USA.

X. Jiang, J. C.-F. Lo, and Z.-L. Yang, Department of Geological Sciences, John A. and Katherine G. Jackson School of Geosciences, 1 University Station, C1100, University of Texas at Austin, Austin, TX 78712-0254, USA. (liang@mail.utexas.edu)